Physics and Imaging in Radiation Oncology 13 (2020) 7–13

Contents lists available at ScienceDirect

Physics and Imaging in Radiation Oncology

journal homepage: www.elsevier.com/locate/phro

Original Research Article

Does an immobilization mask have added value during planning magnetic resonance imaging for stereotactic radiotherapy of brain tumours?

Steven H.J. Nagtegaal[a,*], Astrid L.H.M.W. van Lier[a], Anne A. den Boer[a], Miranda C.A. Kramer[b], Giuseppe Fanetti[c], Wietse S.C. Eppinga[a], Marielle E.P. Philippens[a], Joost J.C. Verhoeff[a], Enrica Seravalli[a]

[a] UMC Utrecht, Department of Radiation Oncology, Utrecht, The Netherlands
[b] UMC Groningen, Department of Radiation Oncology, Groningen, The Netherlands
[c] Centro di Riferimento Oncologico di Aviano (CRO) IRCCS, Aviano, Italy

ARTICLE INFO

Keywords:
Radiation oncology
Brain tumours
MRI
Treatment planning
Immobilization mask

ABSTRACT

Background and purpose: When using an immobilization mask, a magnetic resonance imaging (MRI) head receive coil cannot be used and patients may experience discomfort during the examination. We therefore wish to assess the added value of an immobilization mask during all MRI scans intended for cranial stereotactic radiotherapy (SRT) planning.

Materials and methods: An MRI was acquired with and without a thermoplastic immobilization mask in ten patients eligible for SRT. A planning computed tomography (CT) scan was also made, to which the two MRIs were independently registered. Additionally, the MRI without immobilization was registered to the MRI in mask. On each sequence, gross tumour volume (GTV), the right eye, brain stem and chiasm were delineated. The absolute differences in centre-of-gravity coordinates and Dice coefficients of the volumes of the delineated structures between the two MRIs were compared.

Results: Differences in GTV volume between the two MRIs were low, with median Dice coefficients between 0.88 and 0.91. Similarly, the median absolute differences in centre-of-gravity coordinates between the GTVs, organs at risk and landmarks delineated on the two MRIs were within 0.5 mm. The 95% confidence intervals of the median absolute differences in the three GTV coordinates was within 1 mm, which corresponds to the target volume safety margin used to account for possible errors during the SRT treatment chain.

Conclusions: The effect of scanning a patient without the immobilization mask falls within acceptable bounds of error for the geometrical accuracy of the SRT treatment chain. Consequently, placing the head in treatment position during all MRI scans for patients undergoing radiotherapy of brain metastasis is deemed unnecessary.

1. Introduction

Radiation therapy (RT) is a corner stone in the treatment for brain metastases. High quality imaging is necessary for RT treatment planning, in order to assure that the target volume is adequately identified and delineated. Currently, two imaging modalities are used in the RT workflow of brain metastases, computed tomography (CT) and magnetic resonance imaging (MRI). The CT scan provides electron density information necessary for dose calculations in the currently commercially available treatment planning systems. The MRI is used for anatomical information (especially tumour extent) and is usually acquired shortly before RT delivery as progression and shifting of the lesions over time has been shown to occur in patients with brain metastasis [1]. A contrast-enhanced T1-weighted sequence is the recommended MRI simulation reference image for intracranial stereotactic radiotherapy (SRT) [2]. For delineation purposes, the two image modalities are usually rigidly registered to each other. The accuracy of this registration directly affects the location and size of the target volume and organs at risk (OAR).

During radiation delivery for brain tumours the head of the patient is immobilized in a custom-made thermoplastic mask and head rest. This is done in order to guarantee the reproducibility of the patient's head position between the planning CT and the treatment sessions, as well as to minimize patient's head motion during the sessions themselves (intrafraction motion) [3–6]. In some clinics the MRI examination, prior to RT, is also performed with the patient immobilized in the

* Corresponding author.
E-mail address: s.h.j.nagtegaal-2@umcutrecht.nl (S.H.J. Nagtegaal).

https://doi.org/10.1016/j.phro.2020.02.003
Received 16 September 2019; Received in revised form 13 February 2020; Accepted 21 February 2020

thermoplastic mask, with the goal of minimizing the registration error with the planning CT [2,5]. Reducing registration errors is crucial especially for an SRT workflow, where target volume safety margins as small as 1 mm or even 0 mm are adopted [6,7]. Moreover, using immobilization equipment during examination reduces possible motion artefacts in MR images.

However, using this immobilization mask during the MRI examination comes with two disadvantages. Firstly, patients may experience discomfort while wearing the mask for 30–45 min [8–10]. Despite the material being light and breathing, it may cause feelings of claustrophobia, especially while in an MRI scanner. Secondly, generic flexible MRI receive coils are required to create a setup that combines immobilization and imaging coils because a multi-channel receive head coil does not allow space and fixation for either a head rest or a thermoplastic face mask [11]. Therefore, this type of coils does not allow acquisition of images, such as fluid-attenuated inversion recovery (FLAIR), which require high signal-to-noise ratios and/or depend on acceleration to keep the scan time within an acceptable range [12,13]. Moreover, the flexible coil setup results in more non-uniform receive sensitivity and reduced signal-to-noise ratio compared to a head coil which limits the image quality [2]. For these reasons, it would be desirable to acquire the treatment planning MRIs without the immobilization mask.

In an MR-only RT workflow, the generated synthetic CT (sCT) is also used for dose calculations and at the linac for patient position verification [14]. Therefore, the MRI sequence used to generate the sCT needs to be acquired in treatment position, i.e. with an immobilization mask, in order to have the same patient's head position on the sCT and at the linac. However, the rest of the planning MRI sequences are acquired without immobilization to enable use of the dedicated MR receive head coil which can be used for scan acceleration and improved signal-to-noise ratio.

In this study we assess the accuracy of the registration of (1) the treatment planning MRI with and without an immobilization mask with the planning CT (CT-based workflow) and (2) of the treatment planning MRI without immobilization to the MRI in mask (MR-only workflow), to establish the added value of a mask during the MRI examination.

2. Material and methods

2.1. Patient selection

Ten patients who were referred to the radiotherapy department for SRT of one or two brain tumours were prospectively included. Approval for this study was obtained from the local medical research ethics committee (study number #17/906).

2.2. Imaging

For each patient, the following imaging was performed: 1) a planning CT, 2) a contrast-enhanced T1 3D MRI scan with patient immobilized in a custom made 3-point thermoplastic mask (Civco Medical Solutions, Kalona, Iowa, USA) combined with an individual head support (mask MR), and 3) a contrast-enhanced T1 3D MRI scan without immobilization mask (no-mask MR) [15]. With the immobilization masks a T1 3D, T2 3D FLAIR, diffusion weighted imaging (DWI) spectral presaturation with inversion recovery (SPIR), contrast enhanced T2 turbo spin echo (TSE) and T1 3D were acquired according to the department clinical protocol, without the immobilization mask only a contrast enhanced T1 3D MRI scan was acquired to limit the patient burden. This sequence was chosen for the purpose of the study because it is used to define the target volume and for matching to the planning CT according to the department clinical practice.

The CT scans were helically acquired, on the same day of the MRI, on a Brilliance Big bore scanner (Philips Medical Systems, Best, The Netherlands) with fixed tube potential of 120 kV, 1 mm slice thickness with in-plane resolution varying between 0.7 and 1.0 mm^2. MRI acquisition was performed on a 1.5 T Philips Ingenia scanner (Philips Medical Systems, Best, The Netherlands) using either surface coils (Flex M coils) for the mask MR [16] or a multi-channel Head coil (no-mask MR). MRI scan parameters can be found in Supplementary Table 1. The two MRIs, without and with immobilization mask, were acquired during the same scan session, first the image with immobilization mask and then the no-mask image. Between scans, the patient had to stand up from the table to remove the mask and the receive coils, and to mount the posterior part of the head coil to the table. The average time between the acquisition of the two sequences was 11 min (range: 10–14 min). Patients were given a single dose of gadolinium contrast agent before undergoing the two MRI examinations. Only the contrast enhanced T1 weighted sequence was repeated with the immobilization mask because this sequence is used to define the target volume in line with the recommendations of Paulson [2] and to minimize the patient burden. In Fig. 1 the setup used to acquire the two MRI scans is depicted.

2.3. Image processing

The two MRIs were independently registered to the planning CT (CT-based workflow) and the MRI without immobilization to the MRI in mask (MR-only workflow) by a normalized mutual information algorithm [17] which was restricted to rigid registration according to the department clinical protocol. The clipbox for the registration, which was manually placed for each patient, included the whole patient's skull. Fully automated registration was used without manual adjustments in order to exclude possible subjective errors.

In a previous study [14], the geometrical accuracy of the imaging protocol was already assessed. For this purpose the B_0 inhomogeneity was used according to the method described by Eggers et al. [18]. The high readout bandwidth of the 3D T1w sequence together with the 1.5 T field strength resulted in an average distortion smaller than 1 mm.

The gross tumour volume (GTV) was delineated by three radiation oncologists on both mask MR and no-mask MR scans for each patient. Multiple observers were asked to delineate the target volume to filter out possible delineation uncertainties. Moreover, three OARs were delineated by one radiation oncologist: the brain stem, chiasm and right eye. The eye, brain stem and chiasm were considered because these are important OAR for cranial RT. The choice for left or right eye was arbitrary.

Finally, eight well-defined point-based landmarks were marked by a trained radiation therapy technologist on both scans: 1) the most dorsal point of the cavernous sinus, 2) the most lateral/ventral point of the left ventricle, 3) the most lateral/dorsal point of the right ventricle, 4) optic chiasm, 5) pituitary stalk, 6) external acoustic meatus, 7) attachment of cerebellar tentorium to falx cerebri, 8) sella turcica. For one patient landmarks 1–6 were identified seven times in order to assess the intra-observer error.

2.4. Data collection and statistical analysis

The image quality difference between mask MR and no-mask MR scans was qualitatively evaluated: a radiation oncologist blindly compared the two MRI scans (using the same window/level settings) and stated which had superior image quality for visualizations of the OARs and the GTV. This subjective measure was chosen to assess image quality because the authors feel that this is more clinically relevant measure than other objective measures, i.e. signal-to-noise ratio.

The quality of the registration was quantitatively assessed by looking at the difference in centre-of-gravity coordinates and volumes of the delineated/mark structures on the two MRI scans for the two considered situations, CT-based and MR-only workflow.

For the calculations, the coordinates in the three orthogonal directions of the landmarks and the centre of gravity of the GTV (median of

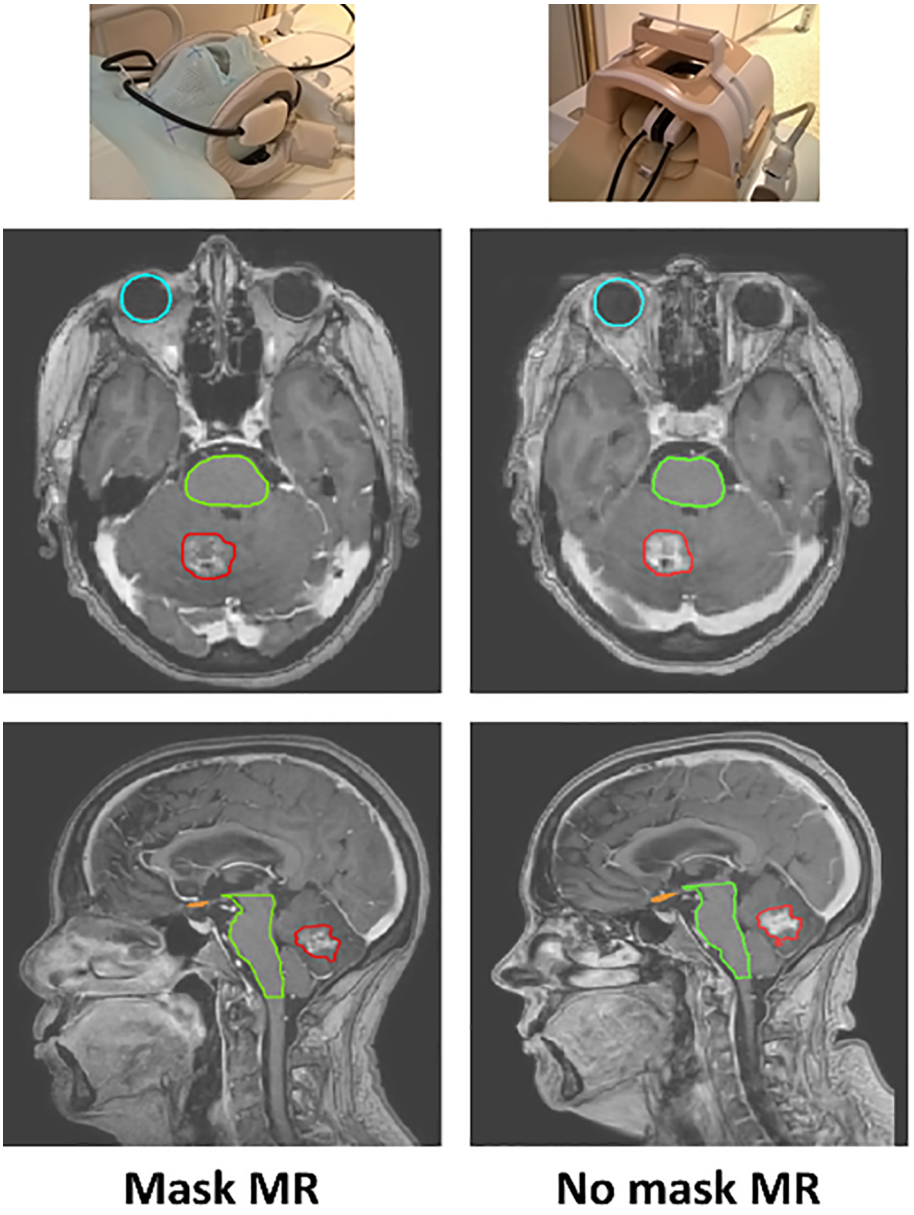

Fig. 1. Setup of MRI scans with and without mask (top row) and the obtained images (bottom rows), with delineated GTV (red), right eye (light blue), brain stem (green), chiasm (orange). (For interpretation of the references to colour in this figure legend, the reader is referred to the web version of this article.)

three observers) and OAR were considered. The centre-of-gravity coordinates were automatically calculated by in-house developed software [17]. Furthermore, the volumes of the delineated GTV and OARs were automatically calculated by the same software.

Absolute differences between the mask MR and no-mask MR scans were calculated by subtracting the coordinates and volumes of the selected regions of interest between the two scans. Additionally, the vectors of the differences in coordinates of the regions of interest were calculated. Individual differences between the two scans were visualized with boxplots for all outcomes, and a Bland Altman plot was made to show the differences in GTV volume relative to mean GTV volume. Finally, differences in GTV delineation between the mask and no-mask MR were compared by calculating the Dice coefficient for each patient, and determining its median and interquartile range (IQR) for the CT-based and MR-only workflows.

Differences on group level were determined with related-samples Wilcoxon signed rank tests, resulting in median differences over all patients. With these, it was tested whether there was a significant difference between the coordinates of the mask and no-mask MR delineated structures, and what the 95% confidence interval (CI) of the found difference was. The tests were performed separately for each coordinate in the three orthogonal directions, as well as for the difference in volume of the GTV and OARs.

Intra-observer concordance of the landmarks coordinates was assessed by the intraclass correlation coefficient (ICC). The GTV inter-observer variance was determined by calculating the range in volume and coordinate differences between observations within patients. Statistical analyses were performed in R 3.5.1 open-source software with the 'irr' package [19].

3. Results

Baseline characteristics of the 10 patients are shown in Table 1.

3.1. Image quality

The no-mask MR image quality was found to be superior in 9 of the 10 cases. Examples of MR images with delineated GTV are shown in

Table 1
Baseline characteristics of included patients.

	Patients (n = 10)
Mean age in years (range)	64 (42–83)
Sex (male)	4
Lesion	
Meningioma	2
Brain metastasis	8
Number of lesions	
1	6
2	4
Location	
Right hemisphere	
Frontal	3
Parietal	3
Temporal	1
Occipital	2
Left hemisphere	
Frontal	1
Occipital	1
Falx cerebri	1
Tentorium	1
Cerebellar peduncle	1
Mean weight in kg (range)	75 (60–95)

Fig. 1. It can be observed that omitting the mask results in a patient's head rotation around the left-right-axis with respect to the scan with the mask.

3.2. Coordinates of GTV and OARs

Differences in coordinates of the GTV and OAR are shown in Fig. 2, and those of the individual landmarks are shown in Fig. 3.

For the CT-based workflow, the related-samples Wilcoxon signed rank tests found significant differences between mask MR and no-mask MR of the following parameters: y-coordinate (corresponding to the anterior-posterior direction) of the GTV for all three observers, x-coordinate of the GTV in one observer, and y-coordinate of the OARs. However, the 95% CI of the found median differences in coordinates was within 1 mm for all regions of interest in all observers (see Supplementary Fig. 1 for a graphical representation of the median differences and their confidence intervals).

For the MR-only workflow, significant differences were found only in the x-coordinate of the GTV in one observer, and in the y-coordinate of the OARs. Other coordinates for GTV and OARs did not significantly differ between the mask and no-mask MRI.

3.3. Volumes of GTV and OARs

Boxplots of the differences in volumes of GTV and OAR between mask MR and no-mask MR (mask MR minus no-mask MR) are shown in Fig. 4. Bland Altman plots of the GTV volume differences between mask MR and no-mask MR are shown in Supplementary Fig. 2.

The median Dice coefficients for differences in GTV delineation between mask and no-mask MR ranged between 0.88 and 0.90 for the CT-based workflow, and 0.88 and 0.91 for the MR-only (see also

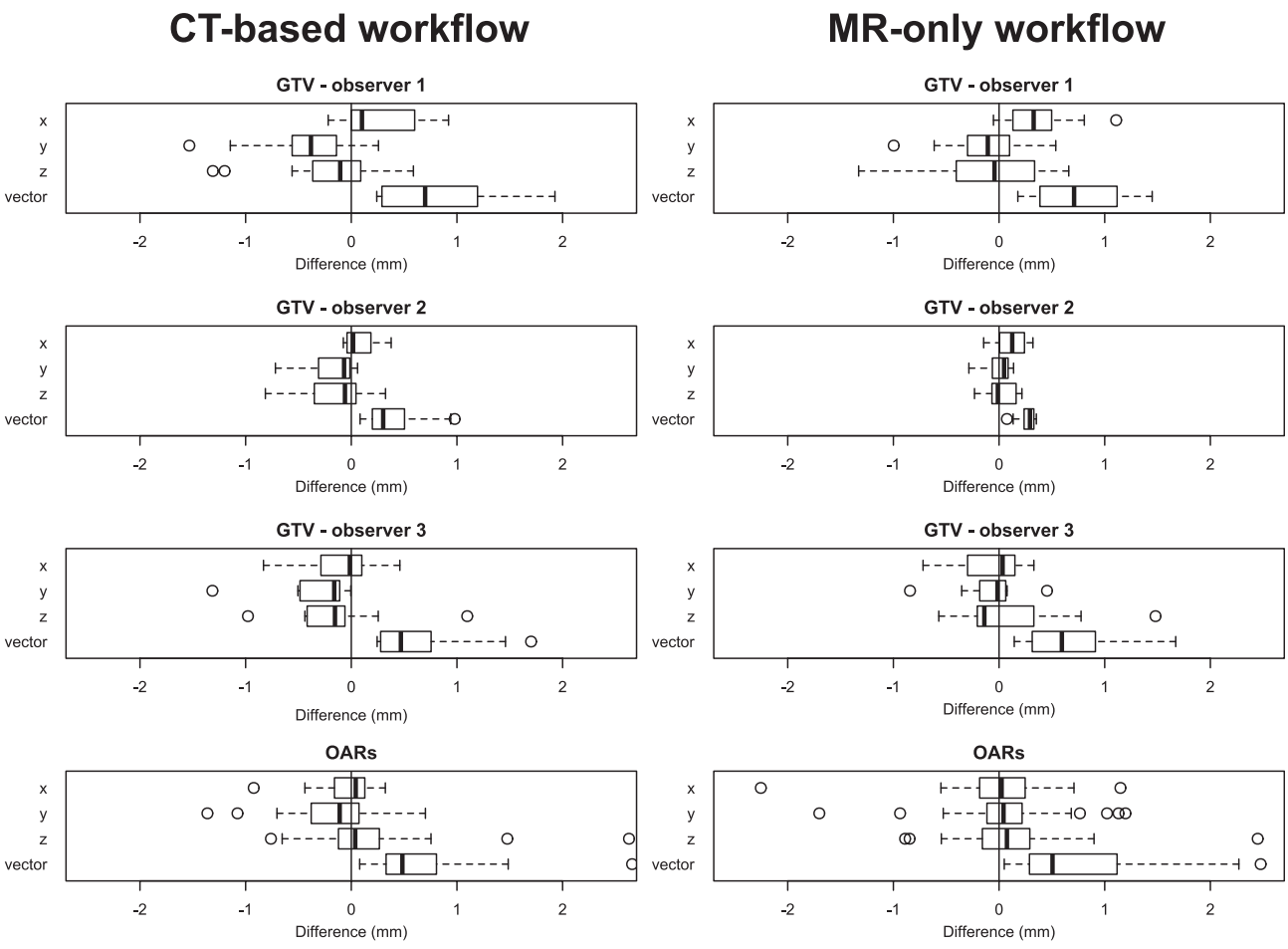

Fig. 2. Boxplots of differences of the centre-of-gravity of GTV and OAR coordinates between mask MR and no mask MR images in the three orthogonal directions, plus their vector lengths (x = right-left, y = anterior-posterior, z = cranio-caudal). The two outliers with more than 2 mm difference are due to intra-observer variation: in both cases an extra CT slice was delineation on one MRI sequence with respect to the other sequence.

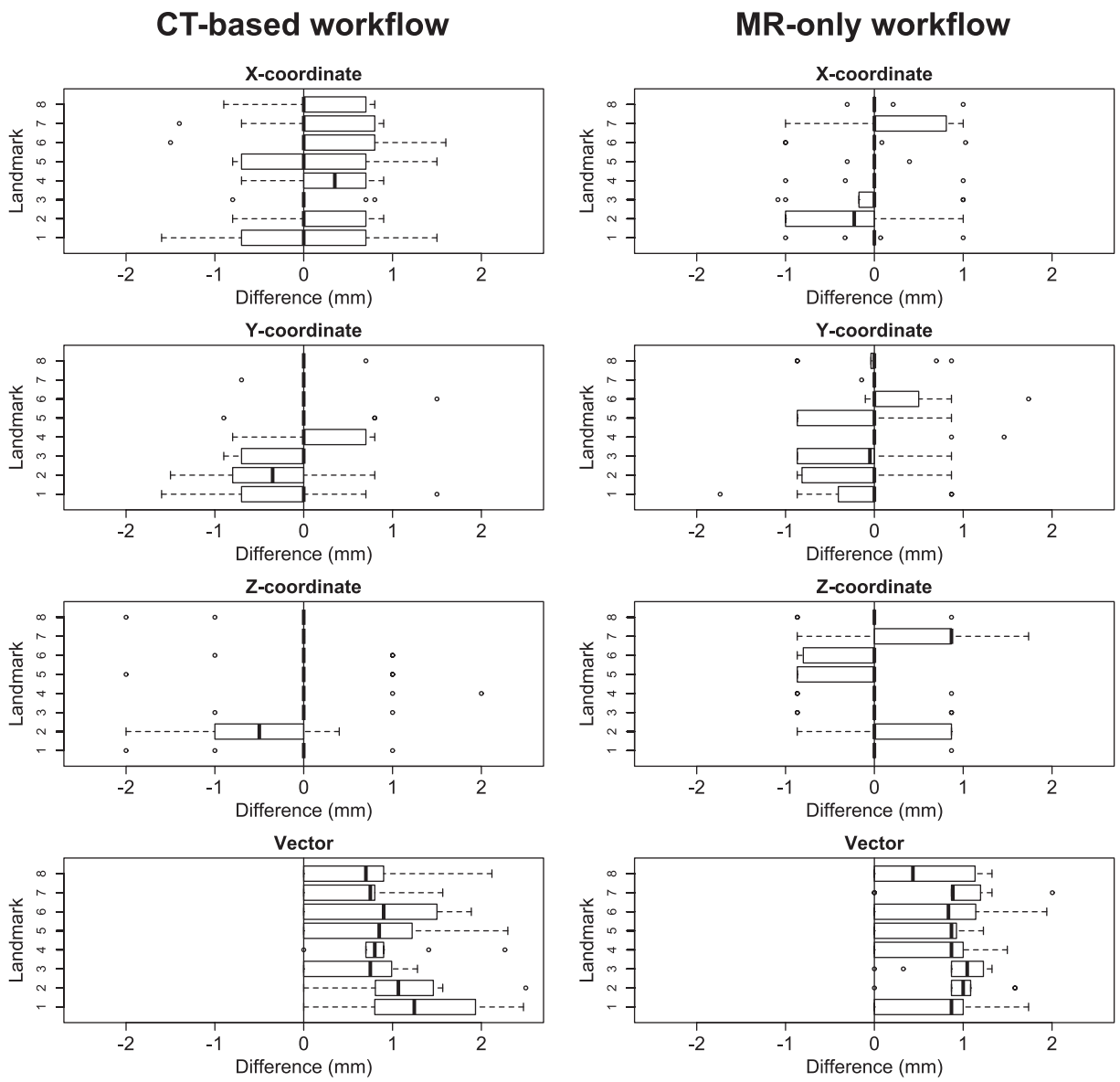

Fig. 3. Boxplots of differences of the landmarks coordinates between mask MR and no mask MR images in the three orthogonal directions, plus their vector lengths (x = right-left, y = anterior-posterior, z = cranio-caudal).

Table 2). For the OARs, the median Dice coefficients were 0.94 for both the right eye and the brain stem. The chiasma had the poorest median Dice, with 0.81 and 0.76 for the CT-based and MR-only workflows, respectively.

For the CT-based workflow, significant differences in GTV volume was found in two observers. The observed median differences were 0.3 cc (95%CI 0.2–0.4) and 0.7 cc (95%CI 0.3–0.9). Comparable results were found for the MRI-only workflow, with significant differences of 0.3 cc (95%CI 0.2–0.5) and 0.7 cc (95%CI 0.4–1.0) for the same two observers. In all cases the volume found in the no-mask MRI was larger than in the mask MRI (Supplementary Fig. 3). For the OARs, no differences were found in either workflow.

3.4. Intra-observer and inter-observer error

The intra-observer variability was negligible, with an ICC of 0.999 (95% CI 0.999–1.000, $p < 0.01$). The range of inter-observer variance was 0.3–1.9 cc for volumes and 0.3–1.5 mm for coordinates in the CT-based workflow. For the MRI-only workflow, these were 0.3–3.7 cc and 0.3–1.6 mm.

4. Discussion

In this study, the differences in registration between the treatment planning MRI scan acquired with and without immobilization mask, both independently rigidly registered to the planning CT (CT-based workflow) and between the MRI without immobilization and the MRI in mask (MR-only workflow) for brain tumours was examined. For all considered regions of interest (landmarks, OARs and GTV), the median absolute difference of the centre-of-gravity coordinates between the two MRIs was found to be less than 1 mm. Similarly, the median differences in GTV volumes ranged from 0.3 to 0.7 cc, which was close to the minimum interobserver variability, and considerably smaller than the maximum interobserver variability (3.7 cc). The Dice coefficients showed a similar favourable result, ranging from 0.88 to 0.91 for the GTV.

This implies that the effect of omitting an immobilization mask during MRI scanning on the overall geometrical accuracy of the RT treatment chain falls within acceptable bounds of error for the geometrical accuracy of SRT delivery. This finding is valid for brain tumours and does not apply to the head and neck area.

Fig. 4. Boxplots of differences in volumes of GTV and OAR between mask MR and no mask MR images (mask MR minus no-mask MR).

Table 2
Median Dice coefficients for the differences between mask MR and no-mask MR.

	Median Dice (IQR) CT-based	Median Dice (IQR) MR-only
GTV – observer 1	0.88 (0.85–0.92)	0.88 (0.86–0.92)
GTV – observer 1	0.90 (0.88–0.94)	0.91 (0.89–0.94)
GTV – observer 1	0.89 (0.88–0.92)	0.88 (0.87–0.93)
Right eye	0.94 (0.92–0.95)	0.94 (0.92–0.95)
Brain stem	0.94 (0.94–0.95)	0.94 (0.94–0.95)
Chiasma	0.81 (0.78–0.84)	0.76 (0.69–0.80)

In the whole RT treatment procedure, several possible sources of error can be identified, each of which adds an error to the final treatment delivery accuracy [7]. Safety margins applied during intracranial SRT to the target volume, which are necessary to accommodate all treatment chain uncertainties, are usually in the order of 1–2 mm. In this work, we have shown that for both OARs and GTV the median absolute coordinate difference of the centre-of-gravity between the mask and no-mask MR scan is within 0.5 mm. For the anatomical landmarks this difference was slightly higher, but still within 1 mm, for which there are two possible explanations. Firstly, the accuracy of the determination of point-based landmarks is more affected by the resolution of the image as well as the accuracy of the manual detection (i.e. by eye) compared to the accuracy of volume delineation. Secondly, the centre-of-gravity approach leads to an averaged location point, whereas the point-based method is confined to discrete location points within the image resolution, which in this study was 1 mm.

The validation of image registration is impeded by the lack of a "gold standard" criterion for registration accuracy tests, as discussed by Speight et al. [20]. As a consequence, the validation process is highly user-dependent and relies on the skills of the user.

When omitting an immobilization device during MRI examination for brain tumors, more attention should be paid to the quality of the image registration. The registration algorithm should also be able to accurately account for rotation differences between the two scans. The anatomical landmarks for registration verification should not be chosen near air-tissue interfaces because of the possible MRI susceptibility artefacts which can cause geometric distortions to the image. Moreover, these landmarks should be chosen to facilitate the assessment of all possible rotations of the patient's anatomy in the three orthogonal directions. Furthermore, correct positioning of all MRI sequences should be validated separately to the planning CT, to assess possible intra-scan motion. An extra registration might be deemed necessary.

When the patient is scanned without an immobilization mask the patient's head has a different inclination than on the planning CT taken with a mask (see Fig. 1), which could affect the delineated structures for MRI with low resolution. In this work, the different inclination did not greatly influence the delineated volumes; an absolute GTV difference of 0.4 cc was found between the two scans, which was in the same order of magnitude as the inter-observer variation in GTV delineation (0.3–3.7 cc).

We foresee two benefits of scanning without an immobilisation device. Firstly, the patient comfort during the MRI sessions will be improved. Secondly, omission of the immobilization mask allows the use of a multi-channel head coil which results in higher image quality and/or reduced scan times. The image quality improvement was also observed in this study, although it was not formally tested. On the other hand, intra-fraction patient motion could affect the images during scanning without the immobilization mask.

When considering an MR-only workflow without online plan adaptation the same immobilization for the patient's head used during treatment delivery should be employed during one sequence of the planning MRI to ensure the same patient position. In fact, the synthetic-CT generated from the planning MR [14] is used for patient position verification at the treatment unit as well. Based on the results of this work it is safe to acquire the rest of the MR protocol without immobilization mask allowing the use of the head coil.

One limitation of this study was the sample size and a non-normal distribution of the variables, meaning that a formal test for equivalence, like the two-one-sided t-tests procedure, could not be performed. Instead, the related-samples Wilcoxon signed rank test was performed, and the confidence interval of the median of the absolute coordinate difference was used to assess whether there were any relevant differences between the mask and no-mask MR. Another limitation is the

relatively large interobserver variability in GTV delineation in two cases. This is likely due to the relative inexperience of one of the observers.

In our study only the contrast-enhanced T1 weighted sequences was considered because this is the only sequence that was without the mask. Prior to that a T1 3D, T2 3D FLAIR, DWI SPIR, contrast enhanced T2 TSE and contrast-enhanced T1 3D were acquired according to the department clinical protocol with the mask on. It was chosen to repeat only one sequence without the mask because 1) the contrast-enhanced T1w scan is used to define the target volume and for matching to the planning CT according to the department clinical practice and 2) in line with the recommendations collected by Paulson et al. [2] to minimize the patient burden. Another consideration is the fact that patients were given a single dose of contrast agent before undergoing the two MRI scans. However, as the total duration between contrast injection and the last scan was less than 30 min, we do not expect this to affect the quality of the scans based on earlier reports [21,22].

In conclusion, this study has shown that the effect of omitting the immobilization mask during MRI imaging on the registration with the planning CT or with the MRI in mask falls within acceptable bounds of error for the geometrical accuracy of SRT delivery. Therefore, head immobilization with a thermoplastic mask during MRI scanning for radiotherapy treatment planning is not necessary resulting in increased patient comfort and allowing the use of multi-channel head coils.

Declaration of Competing Interest

The authors declare that they have no known competing financial interests or personal relationships that could have appeared to influence the work reported in this paper.

Appendix A. Supplementary data

Supplementary data to this article can be found online at https://doi.org/10.1016/j.phro.2020.02.003.

References

[1] Hessen ED, van Buuren LD, Nijkamp JA, de Vries KC, Kong Mok W, Dewit L, et al. Significant tumor shift in patients treated with stereotactic radiosurgery for brain metastasis. Clin Transl Radiat Oncol 2017;2:23–8. https://doi.org/10.1016/j.ctro.2016.12.007.

[2] Paulson ES, Crijns SPM, Keller BM, Wang J, Schmidt MA, Coutts G, et al. Consensus opinion on MRI simulation for external beam radiation treatment planning. Radiother Oncol 2016;121:187–92. https://doi.org/10.1016/j.radonc.2016.09.018.

[3] Thornton AF, Ten Haken RK, Weeks KJ, Gerhadsson A, Correll M, Lash KA. A head immobilization system for radiation simulation, CT, MRI, and PET imaging. Med Dosim 1991;16:51–6. https://doi.org/10.1016/0958-3947(91)90045-4.

[4] Thornton AF, Ten Haken RK, Gerhardsson A, Correll M. Three-dimensional motion analysis of an improved head immobilization system for simulation, CT, MRI, and PET imaging. Radiother Oncol 1991;20:224–8. https://doi.org/10.1016/0167-8140(91)90120-6.

[5] Tryggestad E, Christian M, Ford E, Kut C, Le Y, Sanguineti G, et al. Inter- and intrafraction patient positioning uncertainties for intracranial radiotherapy: a study of four frameless, thermoplastic mask-based immobilization strategies using daily cone-beam CT. Int J Radiat Oncol 2011;80:281–90. https://doi.org/10.1016/j.ijrobp.2010.06.022.

[6] Kocher M, Wittig A, Piroth MD, Treuer H, Seegenschmiedt H, Ruge M, et al. Stereotactic radiosurgery for treatment of brain metastases. A report of the DEGRO Working Group on Stereotactic Radiotherapy. Strahlenther Onkol 2014;190:521–32. https://doi.org/10.1007/s00066-014-0648-7.

[7] Seravalli E, van Haaren PMAMA, van der Toorn PPP, Hurkmans CWW. A comprehensive evaluation of treatment accuracy, including end-to-end tests and clinical data, applied to intracranial stereotactic radiotherapy. Radiother Oncol 2015;116:131–8. https://doi.org/10.1016/j.radonc.2015.06.004.

[8] Li G, Lovelock DM, Mechalakos J, Rao S, Della-Biancia C, Amols H, et al. Migration from full-head mask to “open-face” mask for immobilization of patients with head and neck cancer. J Appl Clin Med Phys 2013;14:243–54. https://doi.org/10.1120/jacmp.v14i5.4400.

[9] Zhao B, Maquilan G, Jiang S, Schwartz DL. Minimal mask immobilization with optical surface guidance for head and neck radiotherapy. J Appl Clin Med Phys 2018;19:17–24. https://doi.org/10.1002/acm2.12211.

[10] Dekker J, Rozema T, Böing-Messing F, Garcia M, Washington D, de Kruijf W. Whole-brain radiation therapy without a thermoplastic mask. Phys Imag Radiat Oncol 2019;11:27–9. https://doi.org/10.1016/j.phro.2019.07.004.

[11] Hanvey S, Glegg M, Foster J. Magnetic resonance imaging for radiotherapy planning of brain cancer patients using immobilization and surface coils. Phys Med Biol 2009;54:5381–94. https://doi.org/10.1088/0031-9155/54/18/002.

[12] de Zwart JA, Ledden PJ, van Gelderen P, Bodurka J, Chu R, Duyn JH. Signal-to-noise ratio and parallel imaging performance of a 16-channel receive-only brain coil array at 3.0 Tesla. Magn Reson Med 2004;51:22–6. https://doi.org/10.1002/mrm.10678.

[13] Parikh PT, Sandhu GS, Blackham KA, Coffey MD, Hsu D, Liu K, et al. Evaluation of image quality of a 32-channel versus a 12-channel head coil at 1.5T for MR imaging of the brain. Am J Neuroradiol 2011;32:365–73. https://doi.org/10.3174/ajnr.A2297.

[14] Dinkla AM, Wolterink JM, Maspero M, Savenije MHF, Verhoeff JJC, Seravalli E, et al. MR-only brain radiation therapy: dosimetric evaluation of synthetic CTs generated by a dilated convolutional neural network. Int J Radiat Oncol 2018;102:801–12. https://doi.org/10.1016/j.ijrobp.2018.05.058.

[15] Houweling AC, van der Meer S, van der Wal E, Terhaard CHJ, Raaijmakers CPJ. Improved immobilization using an individual head support in head and neck cancer patients. Radiother Oncol 2010;96:100–3. https://doi.org/10.1016/j.radonc.2010.04.014.

[16] Verduijn GM, Bartels LW, Raaijmakers CPJ, Terhaard CHJ, Pameijer FA, van den Berg CAT. Magnetic resonance imaging protocol optimization for delineation of gross tumor volume in hypopharyngeal and laryngeal tumors. Int J Radiat Oncol Biol Phys 2009;74:630–6. https://doi.org/10.1016/j.ijrobp.2009.01.014.

[17] Bol GH, Kotte ANTJ, van der Heide UA, Lagendijk JJW. Simultaneous multi-modality ROI delineation in clinical practice. Comput Meth Programs Biomed 2009;96:133–40. https://doi.org/10.1016/j.cmpb.2009.04.008.

[18] Eggers H, Brendel B, Duijndam A, Herigault G. Dual-echo Dixon imaging with flexible choice of echo times. Magn Reson Med 2011;65:96–107. https://doi.org/10.1002/mrm.22578.

[19] R Core Team. R: A language and environment for statistical computing. R Found Stat Comput 2017.

[20] Speight R, Schmidt MA, Liney GP, Johnstone RI, Eccles CL, Dubec M, et al. IPEM topical report: a 2018 IPEM survey of MRI use for external beam radiotherapy treatment planning in the UK. Phys Med Biol 2019;64:175021https://doi.org/10.1088/1361-6560/ab2c7c.

[21] Jeon J-Y, Choi JW, Roh HG, Moon W-J. Effect of imaging time in the magnetic resonance detection of intracerebral metastases using single dose gadobutrol. Korean J Radiol 2014;15:145. https://doi.org/10.3348/kjr.2014.15.1.145.

[22] Kushnirsky M, Nguyen V, Katz JS, Steinklein J, Rosen L, Warshall C, et al. Time-delayed contrast-enhanced MRI improves detection of brain metastases and apparent treatment volumes. J Neurosurg 2016;124:489–95. https://doi.org/10.3171/2015.2.JNS141993.